CellPress

Structure
Article

Structural Basis for Phosphoinositide Substrate Recognition, Catalysis, and Membrane Interactions in Human Inositol Polyphosphate 5-Phosphatases

Lionel Trésaugues,[1,6] Camilla Silvander,[1,4,6,*] Susanne Flodin,[1] Martin Welin,[1] Tomas Nyman,[1] Susanne Gräslund,[1] Martin Hammarström,[1,5] Helena Berglund,[1] and Pär Nordlund[1,2,3,*]

[1]Structural Genomics Consortium, Karolinska Institutet, 17177 Stockholm, Sweden
[2]Division of Biophysics, Department of Medical Biochemistry and Biophysics, Karolinska Institutet, 17177 Stockholm, Sweden
[3]Centre for Biomedical Structural Biology, School of Biological Sciences, Nanyang Technological University, 637551, Singapore
[4]Present address: Sprint Bioscience, Teknikringen 38A, 114 28 Stockholm, Sweden
[5]Present address: Pfizer Health AB, Box 108, 64522 Strägnäs, Sweden
[6]Co-first author
*Correspondence: camilla.silvander@sprintbioscience.com (C.S.), par.nordlund@ki.se (P.N.)
http://dx.doi.org/10.1016/j.str.2014.01.013

SUMMARY

SHIP2, OCRL, and INPP5B belong to inositol polyphosphate 5-phophatase subfamilies involved in insulin regulation and Lowes syndrome. The structural basis for membrane recognition, substrate specificity, and regulation of inositol polyphosphate 5-phophatases is still poorly understood. We determined the crystal structures of human SHIP2, OCRL, and INPP5B, the latter in complex with phosphoinositide substrate analogs, which revealed a membrane interaction patch likely to assist in sequestering substrates from the lipid bilayer. Residues recognizing the 1-phosphate of the substrates are highly conserved among human family members, suggesting similar substrate binding modes. However, 3- and 4-phosphate recognition varies and determines individual substrate specificity profiles. The high conservation of the environment of the scissile 5-phosphate suggests a common reaction geometry for all members of the human 5-phosphatase family.

INTRODUCTION

Membrane-bound phosphoinositides (PtdInsP) and the corresponding soluble inositol phosphates (InsP) regulate a multitude of cellular processes including cell proliferation, synaptic vesicle recycling, receptor signaling, and actin polymerization (Di Paolo and De Camilli, 2006; Michell, 2008). They consist of a glycerol-phospholipid linked through a phosphodiester bond to the hydroxyl in position 1 of a *myo*-inositol molecule. Hydroxyls in positions 3, 4, and 5 on the *myo*-inositol ring can be phosphorylated by kinases, thus generating the seven possible isoforms that have so far been identified in higher eukaryotes. These phosphorylation events can be reverted by the antagonist action of specific phosphatases. The consequence is that each phosphorylated isoform mediates specific signaling pathways while also being an intermediate in the production of other phosphorylated isoforms (reviewed in Hakim et al., 2012 and Maffucci, 2012). For example, PtdIns(4,5)-bisphosphate is involved in vesicle trafficking (Martin, 2001), ion-channel regulation (Gamper and Shapiro, 2007), endocytosis (Poccia and Larijani, 2009), exocytosis (Eberhard et al., 1990), actin polymerization (Hartwig et al., 1995; Tolias et al., 2000), and is the precursor of PtdIns(3,4,5)-triphosphate through the action of type I phosphoinositide 3-kinase (PI3K; Vanhaesebroeck et al., 1997).

The variety of processes regulated by phosphoinositides is illustrated by the large spectrum of diseases in which they have been implicated, such as cardiovascular diseases, diabetes, neurological diseases, ciliopathies, and cancers (Conduit et al., 2012; Hakim et al., 2012). Phosphatidylinositol 3-kinases (PI3Ks) are frequently mutated in human cancers and the PIK3 opposing phosphatase PTEN is the second most commonly mutated tumor suppressor after p53 (Ligresti et al., 2009; Liu et al., 2009; Samuels et al., 2004; Yin and Shen, 2008). Myotubularins, which catalyze the hydrolysis of the 3-phosphate on phosphoinositides, are mutated in X-linked centronuclear myopathy and demyelinating Charcot-Marie Tooth neuropathies and are also connected to cancers, epilepsy, and obesity (Amoasii et al., 2012; Azzedine et al., 2003; Bolino et al., 2000; Laporte et al., 1996; Senderek et al., 2003). Consequently, several proteins involved in phosphoinosite-based signaling constitute important targets for therapeutic intervention (Blunt and Ward, 2012; McCrea and De Camilli, 2009; Moses et al., 2009; Suwa et al., 2010a; Waugh, 2012).

The inositol polyphosphate 5-phosphatases (5-phosphatases) regulate phosphoinositide signaling by hydrolyzing the 5-phosphate position of the inositol ring of both soluble inositol phosphates and membrane-bound phosphoinositides (primarily PtdIns(3,4,5)P3, PtdIns(4,5)P2, and PtdIns(3,5)P2), with different substrate preferences (Astle et al., 2007). This family comprises ten members in mammals that share the catalytic 5-phosphatase domain. Five-phosphatases play important roles in human health (Ooms et al., 2009). The 5-phosphatase OCRL is responsible for the oculocerebrorenal syndrome of Lowe, which leads to neurological and renal defects (Attree et al., 1992). Mutations in OCRL also cause Dent disease, which, like Lowes syndrome,

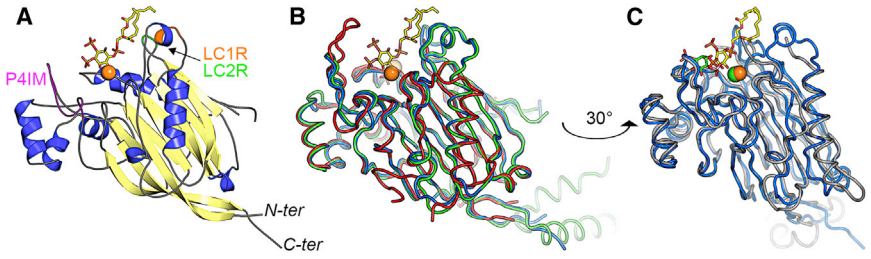

Figure 1. Structure of Complex between INPP5B-cd and diC8PtdIns(3,4)P2: Overall View and Comparison with SHIP2, OCRL, and SPsynaptojanin

(A) Ribbon diagram of INPP5B-cd bound to diC8PtdIns(3,4)P2. Mg^{2+} ion is shown as an orange sphere. Motifs LC1R, LC2R, and P4IM are colored respectively orange, green and purple.

(B) Superimposition of INPP5B-cd/diC8PtdIns(3,4)P2 complex (blue), SHIP2-cd (red), and OCRL-cd (green) Cα traces.

(C) Superimposition of INPP5B-cd/diC8PtdIns(3,4)P2 complex (blue) and SPsynaptojanin-cd bound to inositol (1,4)-bisphosphate. Carbon atoms of diC8PtdIns(3,4)P2 complex and of inositol (1,4)-bisphosphate are yellow and green, respectively. Mg^{2+} ion in INPP5B-cd is shown as an orange sphere, Ca^{2+} ion in SPsynaptojanin-cd as a green sphere.

See also Figure S2 for the location of a putative Ca^{2+} ion observed in the structure of apo-INPP5B-cd.

is an X-linked disorder characterized by kidney failure (Hoopes et al., 2005). To date, about 200 different mutations have been identified in OCRL, most of the missense mutations being located in the 5-phosphatase domain of the protein (Pirruccello and De Camilli, 2012; Zhang et al., 2013). OCRL shares 44% sequence identity with INPP5B and the function of INPP5B and OCRL is likely overlapping (Hellsten et al., 2001; Jänne et al., 1998). The 5-phosphatase SHIP2 negatively regulates insulin-mediated signaling (Dyson et al., 2005), and mice deficient in SHIP2 are resistant to diet-induced obesity (Sleeman et al., 2005). SHIP2 is therefore potentially an interesting drug target for obesity and type 2 diabetes. Mutations in the 5-phosphatase domain of INPP5E have also been identified in the Joubert syndrome type of ciliopathy (Bielas et al., 2009).

Despite many links to disease, the understanding of important aspects of phosphoinositide signaling is still limited. At the protein level, the molecular basis for how substrate recognition and membrane interactions control specificity and activity remains rudimentary for most of the enzyme families of these pathways. The only structure of a 5-phosphatase catalytic domain previously reported is that of *Schizosaccharomyces pombe* synaptojanin (SPsynaptojanin), which revealed a fold similar to that of Mg^{2+}-dependent endonucleases (Tsujishita et al., 2001). The structure was determined in complex with a soluble inositol(1,4)P2 product and thus did not provide any information on how the 5-phosphatases are able to accommodate the lipid moieties of their substrates. In addition, the orientation of inositol(1,4)P2 in the active site of SPsynaptojanin does not facilitate proper modeling of an intact substrate due to steric clashes with the region expected to accommodate the 5-phosphate. Thus, whereas the current model gives a rough estimation on the region that mediates the natural ligand, detailed information concerning substrate position and orientation, interactions between the protein and the fatty acid part of the phosphoinositides, and the catalytic mechanism in the 5-phosphatase family are not available. Understanding these aspects is essential to provide a link between the missense mutations that have been identified in the 5-phosphatase catalytic domains and the diseases they are responsible for. This is exemplified by the phenotypical differences that exist between Lowe syndrome and the milder Dent disease that can be both caused by mutations targeting the catalytic domain of OCRL. Currently, the incomplete model of protein/ligand interactions in the 5-phosphatase family does not allow discrimination between effects caused by a destabilizing mutation and effects due to alterations either in the catalytic machinery or in the ligand-binding site.

To answer these points as well as to understand the molecular basis for membrane interaction in the human 5-phosphatase family, we have determined structures of the catalytic domains of the human 5-phosphatases SHIP2, OCRL, and INPP5B, the latter in complex with two PtdInsP products. These studies give a detailed view of the catalytic machinery and structural features involved in substrate recognition for key members of the human 5-phosphatase family and revealed striking differences in the substrate binding-mode compared to what has previously been suggested from the SPsynaptojanin structure.

RESULTS

Overall Structures of OCRL and INPP5B Catalytic Domains

Useful crystals of the INPP5B and OCRL catalytic domains (INPP5B-cd and OCRL-cd) were obtained after extensive screening of constructs expressing soluble and stable protein using the strategy described by Gräslund et al. (2008). These constructs lack their C-terminal Rho-GAP domains and their N-terminal PH domains, the latter being responsible for the targeting of OCRL to endocytic clathrin-coated pits (Erdmann et al., 2007) mediated through interaction with both clathrin and endocytic clathrin adaptor AP-2 (Ungewickell et al., 2004), whereas its function remains unknown in INPP5B (Mao et al., 2009). The purified catalytic domains were active toward phosphoinositide substrates in vitro (see below). First a 2.65 Å resolution structure of INPP5B-cd was determined in the presence of high Mg^{2+} concentration (200 mM Mg^{2+}), revealing an overall fold similar to the SPsynaptojanin catalytic domain (Protein Data Bank [PDB] number 1I9Y, root-mean-square deviation [rmsd] 1.2 Å for 273 superimposed residues, sequence identity of 34%; for sequence alignment, see Figure S1 available online). The fold is composed of a β sandwich, which is lined by several α helices. Subsequently, structures of INPP5B in complex with product analogs were determined (Figure 1A). A tentative catalytic Mg^{2+} ion was found in the active site of all INPP5B structures. A residual density that could not be attributed to either protein or water molecules was observed in apo-INPP5B-cd maps at Asp414, ca 15 Å from the catalytic Mg^{2+} ion. Its size and coordination environment looked similar to what can be expected of a Ca^{2+} ion (Figure S2; this is the identity in the apo-INPP5B-cd model deposited to the

PDB). Despite extensive efforts, but hampered by the relative instability of the produced protein, we have not been able to conclusively characterize either the nature of this ion or its potential role in the function of INPP5B.

The structure of OCRL-cd was determined at 3.13 Å resolution using molecular replacement with INPP5B-cd as a search model (Figure 1B). The rmsd between OCRL-cd and the INPP5B-cd structures is in the range of 0.7–0.8 Å. The construct of OCRL carries longer C-and N-terminal extensions, where ca 30 C-terminal residues are ordered forming a small two-helix coiled-coiled domain. An Mg^{2+} and a phosphate ion are found in the active site of OCRL. The structure of SHIP2 will be discussed below. Data collection and refinement statistics are shown in Table 1.

To verify the integrity of the constructs used for structural studies, we also assayed the OCRL-cd and the INPP5B-cd constructs, as well as several other human 5-phosphatases for activity using the malachite green assay to monitor phosphate release from diC8PtdInsP substrates. diC8PtdInsPs are soluble analogs of phosphoinositides, having identical head groups but shorter eight-carbon aliphatic chains. All proteins were active against two different substrate analogs, diC8PtdIns(3,4,5)P3 and diC8PtdIns(4,5)P3, albeit with different activity profiles (Figure 2B). We noted that, with the exception of SHIP2, the molecular activity of the 5-phosphatases we assayed were in the same range. Possibly our assay conditions were not optimal for SHIP2, or its low activity (relatively to the other 5-phosphatases present in our study) could be either due to the strong requirement of its N- and C-terminal domains to reach optimal activity or might be a specificity intrinsic to this enzyme that by many points differ from the consensus 5-phosphatases as discussed later in the article.

Recognition of Phosphoinositide Substrates in INPP5B

Extensive diffraction screening of crystals obtained in co-crystallization experiments of INPP5B-cd with diC8PtdIns(3,4,5)P3 yielded two crystals giving data of sufficient quality for structural analysis. The refined structures contained two different hydrolysis products, diC8PtdIns(4)P and diC8PtdIns(3,4)P2. We attribute the presence of two different hydrolysis products to different storage times of the crystals in their growth containers. The binding modes of the two products are virtually identical in the lipophilic region of the substrate as well as for the 1-P unit, whereas the position of the inositol ring and 4-phosphate groups overlap albeit having slightly different orientations in the two structures (Figures 3A and 3B).

The substrates bind to one terminus of the β sandwich where the substrate interactions are made by several loops and short helices connecting the β strands (Figure 1A). The aliphatic region of the diC8PtdInsP products is primarily interacting with a patch composed of two hydrophobic loops: one including Phe311, Phe312, and Phe313, termed lipid chain 1 recognition motif (LC1R-motif); and a second loop being composed of Ile373, Met374, and Met377, termed lipid chain 2 recognition motif (LC2R-motif; Figure 3C).

The 1-P group of the substrate constitutes, together with the inositol ring, the conserved polar moiety of all phosphoinositide substrates and is expected to be a key unit for substrate recognition. In the INPP5B-cd product complexes, the 1-P moiety is recognized by direct hydrogen bonds with the side chains of Asn379 and Lys380 (Figure 3C). Several water molecules, stabilized by protein coordination, also make hydrogen bonds with 1-P (see LIGPLOT diagram in Figure 3D). The only direct recognition of the inositol ring in the product complexes is by the Ala403 side chain where the β carbon is lining the ring (Figures 3A and 3D), whereas the 6-OH group in the product complexes is coordinated by a protein-bound water molecule (Figure 3D). In the product structures of INPP5B-cd, the 4-P group is pinned down in the active site by extensive interactions with the protein through a conserved structural pattern we term the P4-interacting-motif (P4IM), composed of Tyr502, Lys503, Arg518, and Lys 516, as well as a protein coordinated water molecule. In the PtdIns(3,4)P2 complex of INPP5B, the 3-P position is relatively exposed into the solvent but makes a hydrogen bond to His404 (Figure 3A). The fact that INPP5B exhibits extensive interactions with the 4-P group explains its preference for PtdIns(4,5)P2 and PtdIns(3,4,5)P3, and inability to hydrolyse PtdIns(5)P and PtdIns(3,5)P2 (Schmid et al., 2004).

Superposition with the structure of SPsynaptojanin complexed to Ins(1,4)P2 reveals that the metal ions superimpose closely and the products are located in the same cleft, but that the orientation of the inositol moieties of the ligands shows significant differences (Figures 1C and 5I). Whereas the 4-Ps of both products are separated by only 1.8 Å and thus exhibit a similar binding mode mediated by conserved residues, the inositol moieties are rotated relative to each other by approximately 100°, so that their 1-Ps are projected to be 10.3 Å apart (Figure 5I).

Interactions with Scissile Phosphate and Catalytic Mechanism

To gain further insights into substrate recognition and the catalytic mechanism, we initially attempted to trap a nonhydrolyzed substrate complex of INPP5B, but these attempts were not successful. However, the very similar structures of the PtdIns(3,4)P2 and PtdIns(4)P complexes in INPP5B, together with the comprehensive interactions made in the active site including conserved amino acids, suggest that the products can serve as good model for the binding of PtdIns substrates. The subsequent revelation of a well-defined phosphate ion in the structure of OCRL in the region where the 5-P moiety and the 5-phosphate product are expected to bind allowed us to determine the position of the scissile phosphate relative to the inositol ring in the substrate. When overlaying PtdIns(4)P bound-INPP5B-cd and phosphate bound-OCRL-cd, the distance between the departing 5-OH and one of the oxygen atoms of the phosphate ion is only 0.6 Å (Figure 4A); therefore, we can consider that the free phosphate in OCRL-cd structure mimics the position of the 5-phosphate in the substrate.

The 5-P binds in a pocket containing six residues that are highly conserved in the 5-phosphatases (Asn379, Lys380, His400, Asp447, Asn449, and His549 in INPP5B; Figure 4A). At this position, the 5-P interacts directly with Mg^{2+} and also makes direct contacts with His400, His549, Asn449, and Asp 447.

Sequence similarities and mutagenesis studies support that the 5-phosphatases are distant homologs of apurinic/apyrimidic (AP) endonucleases and might have a related mechanism for phosphoryl transfer (Communi et al., 1996; Jefferson and

Table 1. Data Collection and Refinement Statistics

	INPP5B				
Characteristics	Apo	PtdIns-4-P1 bound	PtdIns-3,4-P2 bound	SHIP-2	OCRL
Protein Data Bank number	3N9V	3MTC	4CML	3NR8	4CMN
Data collection					
Synchrotron	Diamond	ESRF	MaxLab	BESSY	Diamond
Beamline	I03	ID29	I911-2	BL14.1	I03
Wavelength (Å)	0.96860	0.97908	1.03796	0.91841	0.97920
Resolution range (Å)[a]	72.55–2.65 (2.79–2.65)	94.51–2.40 (2.53–2.40)	29.89–2.30 (2.42–2.30)	44.77–2.80 (2.95–2.80)	103.78–3.13 (3.30–3.13)
Space group	$I2_12_12_1$	$P2_13$	$P2_13$	$P12_11$	$P4_132$
Unit-cell dimensions (Å)	a = 96.16	a = 133.76	a = 133.66	a = 44.80	a = 146.77
	b = 110.66	b = 133.76	b = 133.66	b = 61.18	b = 146.77
	c = 159.38	c = 133.76	c = 133.66	c = 114.32	c = 146.77
Unit-cell angles (°)	–	–	–	β = 91.9	–
Completeness (%)[a]	99.9 (99.9)	99.8 (99.9)	99.9 (100.0)	99.6 (99.5)	100.0 (100.0)
Unique reflections	25,062	31,417	35,595	15,338	10,068
Mean (I)/SD(I)[a,b]	11.9 (2.1)	11.1 (2.0)	12.5 (2.5)	7.9 (2.0)	55.6 (6.5)
Redundancy[a]	4.6 (4.7)	4.8 (4.5)	5.5 (5.6)	4.6 (4.6)	40.5 (42.4)
R_{meas} (%)[a,c]	8.8 (69.8)	10.2 (79.1)	10.0 (71.2)	17.1 (81.2)	6.2 (80.1)
Refinement					
Resolution range (Å)[a]	53.66–2.65 (2.77–2.65)	47.29–2.40 (2.46–2.40)	28.5–2.30 (2.36–2.30)	20.0–2.80 (2.87–2.80)	48.92–3.13 (3.30–3.13)
R_{cryst} (%)[a,d]	19.1 (26.3)	17.2 (27.0)	17.6 (32.9)	21.6 (32.1)	21.0 (24.5)
R_{free} (%)[a,e]	23.1 (33.1)	20.5 (36.9)	19.9 (37.3)	27.2 (40.2)	26.3 (35.1)
Model content					
Protein atoms	4,645	2,538	2,510	4,791	2,690
Ligand atoms	0	43	47	0	17
Metal atoms	4	1	1	0	1
Water molecules	57	225	320	36	4
Wilson B factors (Å^2)	79.40	54.00	45.50	59.70	106.14
Average B factors (Å^2)					
Protein atoms	74.10	54.08	34.34	41.49	114.53
Ligand atoms		72.46	54.92	–	114.22
Metal atoms	79.42	83.55	40.05	–	128.18
Water molecules	57.75	61.24	46.24	39.43	76.59
Rmsd bonds (Å)	0.011	0.010	0.008	0.009	0.006
Rmsd angles (°)	1.255	1.278	1.243	1.142	0.997
Ramachandran plot (%)[f] (favored, outliers)	97.2, 0	97.1, 0.3	97.1, 0.7	93.58, 0	95.2, 0.3

[a]Numbers in parentheses represent outermost shell.
[b]Mean (I)/SD(I) is the mean ratio for all reflections of < Ih > /sd < Ih > where, for each unique reflection h, < Ih > is the weighted mean of measured Ih and sd < Ih > is the mean of estimated error sd(I).
[c]$R_{meas} = \sum_h \left(\frac{nh}{nh-1}\right) \sum_l |Ihl - \langle Ih \rangle| / \sum_h \sum_l \langle Ih \rangle$
[d]$R_{cryst} = \sum |F_{obs} - F_{calc}| / \sum |F_{obs}|$,
where Fobs and Fcalc are respectively the observed and calculated structure factors.
[e]R_{free} is the same as R_{cryst} but based on a subset of 5% (4.58%, 4.9%, and 10% for Apo-INPP5B, SHIP-2, and OCRL, respectively) of reflections omitted during refinement.
[f]Values computed by Molprobity (Chen et al., 2010).

Majerus, 1996; Whisstock et al., 2000). The detailed mechanism of the hydrolysis reaction mediated by AP endonucleases is still being debated and different models have been proposed. These models include mechanisms involving either one or two Mg^{2+} ions, or alternatively one moving Mg^{2+} ion (Beernink et al., 2001; Gorman et al., 1997; Mol et al., 2000).

In the "single-metal mechanism," a hydroxide produced by Asp210 (Asp447 in INPP5B) would perform a nucleophilic attack

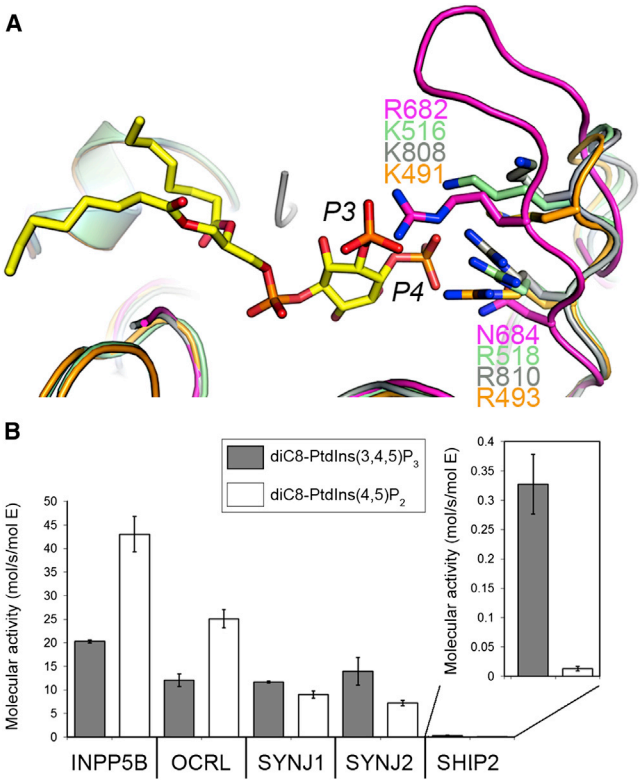

Figure 2. Structural Determinants of the Specificity of the Different 5-Phosphatases

(A) Comparison in the P4IM motif between INPP5B-cd (green), SHIP2-cd (magenta), OCRL-cd (copper), and SPsynaptojanin-cd (gray). diC8PtdIns(3,4)P2 from INPP5B-cd complex structure is depicted as sticks with its phosphate labeled in italic.

(B) Activity profiles of 5 human PtdIns 5- phosphatases monitoring hydrolysis of diC8PtdIns(3,4,5)P3 and diC8PtdIns(4,5)P2. The concentration of substrate was 50 μM and the concentration of enzyme was 3 nM (INPP5B, OCRL), 6 nM (SYNJ1, SYNJ2), or 100 nM (SHIP2). The results are presented as means ± SD of triplicate determinations.

See also the alignment of the ten human members of the 5-phosphatases presented in Figure S1.

on the phosphate and the transition state would be stabilized by a metal coordinated by Asp70 (Asn275) and Glu96 (Glu403), His 309 (His549) being involved in the orientation and polarization of the phosphate (Figures 4B and S3A; Mol et al., 2000). Then, a complex between APE1 and two metals was produced following crystallization under basic conditions. In this model, the hydroxide performing the nucleophilic attack is coordinated by one metal (labeled B in Figure 4C) that might also stabilize the transition state. The second metal (labeled A in Figure 4C) would also either stabilize the transition state or the O3′ departing group (Beernink et al., 2001). Molecular dynamics studies have recently proposed an alternative version of this model in which a single metal would move from site B to site A during the catalytic cycle and would help to generate the hydroxyl in the first part of the reaction while retaining the product in the second part (Figures 4C and S3B; Oezguen et al., 2007).

Currently, there is still controversy about the biological existence of sites A and B. Lipton et al. (2008) conclude that only site A exists when, on the other hand, complementary studies by Oezguen et al. (2011) revealed that the presence of a metal in site A only would destabilize the complex between APE1 and DNA.

Superimposition of the structures of the different 5-phosphatases with APE1, either complexed with the products of the reaction and one or two metals, revealed that the active sites of both enzymes are highly conserved (Figures 4B and 4C). In Figure 4B, it is noticeable that both the metals, the departing phosphate groups (the free phosphate present in OCRL-cd structure being used to identify the position of the scissile phosphate in the 5-phosphatase mechanism) and the sugar rings are shifted by 1.6–2.5 Å whereas the position of the residues involved in the chemistry of the reaction are strictly conserved. It is likely that the geometry of the reaction had to be slightly adjusted during the course of the evolution to use a common structure to hydrolyze either a bulky nucleic acid or a relatively small membrane-bound phospholipid. All residues surrounding the position of the scissile phosphate (5-P) and Mg^{2+} ion in the 5-phosphatases are strictly conserved in APE1, with only one exception: Asp70 (in APE1 structures) is replaced by either asparagines (in INPP5B, OCRL, and SPsynaptojanin) or a glycine (SHIP2). The high conservation supports similar reaction geometry during the phosphoryl transfer reaction in the two enzyme families.

The Mg^{2+} ion present in INPP5B-cd and OCRL-cd structures corresponds to the site A metal in APE1 (according to the nomenclature proposed by Beernink et al., 2001). Similarly, in all but one crystal structure of APE1, only site A was occupied by a metal. In line with a recent proposal for APE1, a two-metal or moving metal mechanism is less likely to occur for the 5-phosphatases (Tsutakawa et al., 2013). Instead Mg^{2+} (in site A, as in our structures) is proposed to play a major role to coordinate the phosphate and stabilize highly negatively charged transition state intermediates and the departing product phosphate, while a water molecule is bound and activated in the pocket formed by Asn449 and Asp447 in INPP5B. As in APE1, no residue in the 5-phosphatase structures is located in a position suitable to assist protonation of the departing 5-OH group. Instead, it is likely that the neighboring Mg^{2+} bound water molecule, or a phosphate group (4-P or 5-P) serves as the proton donors, or assists in the proton transfer to the departing 5-OH.

Structure of SHIP2—A Target for Obesity and Type 2 Diabetes

SHIP2 has recently attracted significant attention due to its role in negative regulation of insulin signaling and as a potential drug target for obesity and type 2 diabetes (Sasaoka et al., 2006; Suwa et al., 2010a). SHIP2 has a preference for Ins(1,3,4,5)P4, PtdIns(3,5)P2 and PtdIns(3,4,5)P3 but is unable to mediated hydrolysis of PtdIns(4,5)P2 as shown in Chi et al. (2004), Pesesse et al. (1998), and in Figure 3B. Therefore, it appears to have a stronger requirement for the presence of the 3-P phosphate in the substrate than other members of the 5-phosphatase family. This is consistent with its proposed role as a negative regulator of PtdIns(3,4,5)P3 levels at the plasma membrane, thereby attenuating the Akt pathway-mediated insulin signaling.

SHIP2 is a modular protein composed in addition to its catalytic domain of an N-terminal SH2, C-terminal proline-rich, and

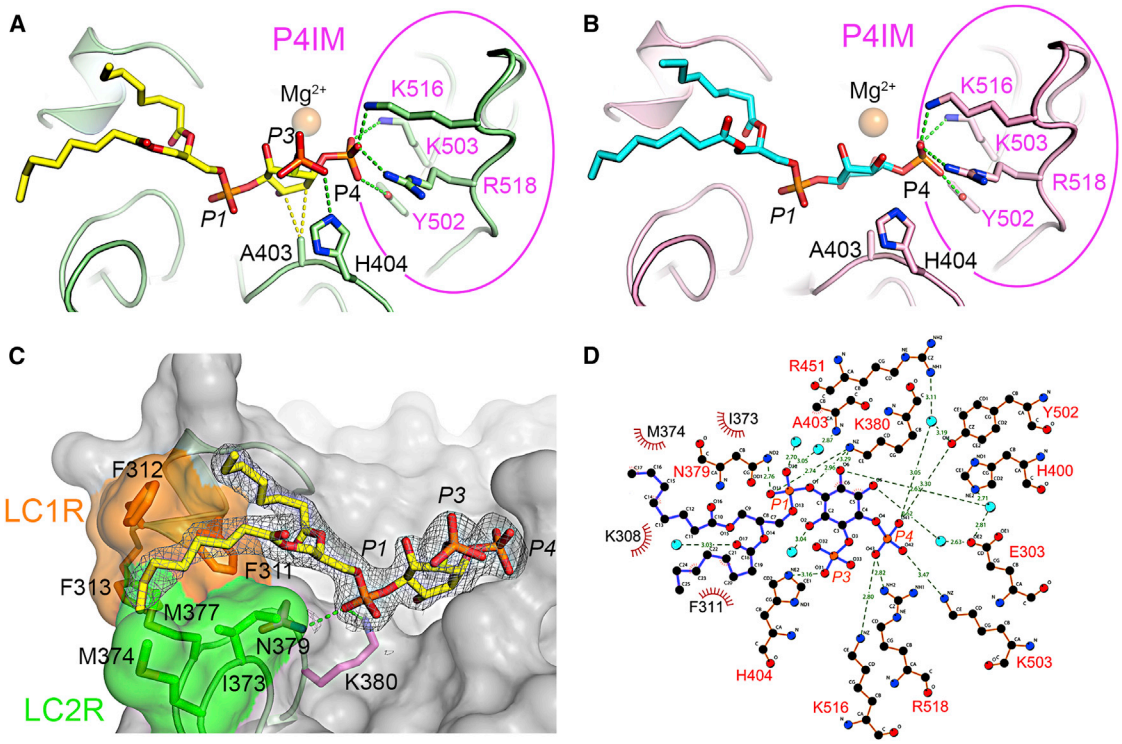

Figure 3. Binding Mode of the Product Analogs to INPP5B-cd

(A and B) Interactions between INPP5B-cd and either diC8PtdIns(3,4)P2 (A) or diC8PtdIns(3)P1 (B): interactions with head group phosphates. Polar and van der Waals interactions between INPP5B-cd and product analogs are shown as yellow and green dashes, respectively. Residues belonging to the P4IM motif are circled in purple.

(C) INPP5B-cd/diC8PtdIns(3,4)P2 binding-mode: interactions with phosphate P1. DiC8PtdIns(3,4)P2 is displayed as sticks with the corresponding 2mFo-DFc electron density contoured at 1 σ. LC1R and LC2R motifs are orange and green, respectively. Interactions between phosphate P1 and INPP5B-cd residues are depicted by green dashes.

(D) Ligplot diagram of interactions between INPP5B-cd and diC8PtdIns(3,4)P2. Protein and ligand covalent bonds are orange and purple, respectively. Water molecules are shown as cyan spheres. H-bonds and salt-bridges are represented by green dashes and hydrophobic interactions by red lines. Distances between two interacting atoms are written in green (in angstroms).

SAM domains. These three particular domains are involved in protein-protein interactions, notably playing a role in membrane-targeting of the enzyme. We have restricted our study to the catalytic domain of SHIP2 (referred as SHIP2-cd).

The structure of apo SHIP2-cd, determined at 2.80 Å resolution, shows a similar overall fold as INPP5B-cd and OCRL (rmsd is 1.2 Å for 265 and 266 superimposed residues, 30.7% and 29.3% sequence identity, respectively) but major local differences in the regions involved in substrate-binding (Figures 1B and 2A). Modeling of the PtdIns(3,4)P3 product into SHIP2 based on the INPP5B complex confirms that most residues interacting with 1-P and 5-P units of the substrate are conserved and are positioned similarly (Figure 4A), suggesting that the general substrate binding mode will be similar. Major differences in the SHIP2 structure, likely to be key for its specific biological function, are found in the P4IM motif. The loop including P4IM is 7 residues longer in SHIP2 than in INPP5B (Figure 2A). This loop is disordered in one of two molecules present in the asymmetric unit. The additional extension in SHIP2 makes this loop quite different than the corresponding loop in INPP5B. In SHIP2, Arg682 and Asn684 are well positioned to interact with both 3-P and 4-P of the substrate.

A recent study based upon analysis of a complex between SHIP2 and a specific competitive inhibitor revealed that, upon binding, the P4IM motif fold over the inhibitor (Mills et al., 2012). Therefore, this loop could similarly fold over the 3-P and 4-P positions of the substrate, thereby allowing more extensive substrate interactions. The interaction between Arg682 and 3-P is likely the driving force of this conformational change, thereby explaining the restricted specificity of SHIP2 (and closest homolog SHIP1) toward substrates harboring phosphates in position 3.

Implications for Substrate Binding in other Human 5-Phosphatases

Our structural analysis, taken together with the conservation of key residues and functionalities, has broader implications for the human 5-phosphatase family. The structural and sequence data suggest that the 5-phosphatases recognize their substrates in a very similar manner, involving several conserved residues interacting with the 1-P, 4-P and 5-P moieties. Lys380, interacting with 1-P, is conserved in all human 5-phosphatases, together with the neighboring Gly381 (See Figure S1 for sequence alignment). The other key residue in 1-P interaction, Asn379, is conserved in all human 5-phosphatases except INPP5E and INPP5A, where

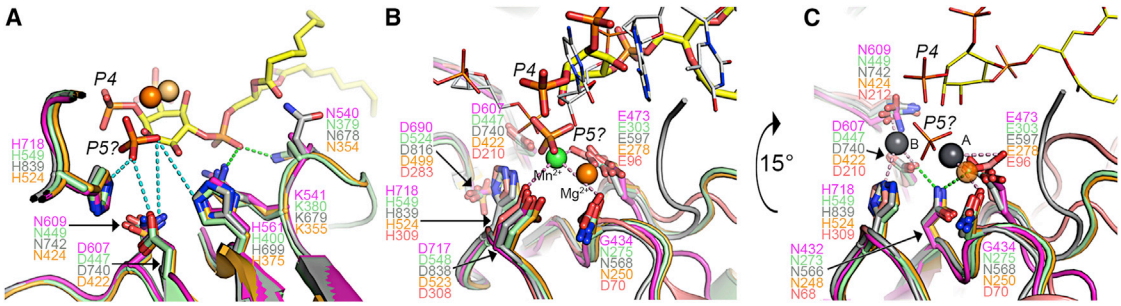

Figure 4. 5-Phosphatases Catalytic Mechanism: Comparison with Representative Human Apurinic/Apyrimidinic Endonuclease, Ape1

(A) Superimposition of INPP5B-cd (green), SHIP2-cd (magenta), OCRL-cd (copper), and SPsynaptojanin-cd (gray) in the active site. The free phosphate present in OCRL-cd structure is depicted as sticks and labeled as "P5." Mg^{2+} ions present in INPP5B-cd/diC8PtdIns(3,4)P2 complex and OCRL-cd are displayed as orange and sand spheres, respectively. Polar interactions between P1, the putative P5 site, and INPP5B-cd residues are shown as dashes.

(B) Superimposition of INPP5B-cd (green), SHIP2-cd (magenta), OCRL-cd (copper), SPsynaptojanin-cd (gray), and Ape1 (salmon) complexed to the two products of its reaction. In addition to the features reproduced from (A), the two nucleic acids present in the Ape1 structure are displayed as thin sticks with their carbon atoms colored white. Mg^{2+} ion (INPP5B-cd structure) and Mn^{2+} (Ape1 structure) are shown as orange and green spheres, respectively.

(C) Superimposition of INPP5B-cd (green), SHIP2-cd (magenta), OCRL-cd (copper), SPsynaptojanin-cd (gray), and Ape1 (salmon) complexed to Pb^{2+} ions. The two Pb^{2+} ions present in the Ape1 structure are dark gray.

See also the two possible catalytic mechanisms presented in Figure S3.

it is replaced by Thr and Arg, respectively. INPP5A only transform soluble InsP substrates, and an additional positive charge at this position might provide additional 1-P interactions. Ala403, which recognizes the inositol ring, is conserved as a small side chain in most human family members (as alanine or serine) indicating similar interactions with substrate inositol groups.

Most of the human 5-phosphatases prefer substrates phosphorylated at the 4-position. Lys516 interacting with the 4-P positions is conserved in all 5-phosphatase family members except INPP5A (Asp), but is positioned differently in SHIP2, as revealed by our structure (Figure 2A). Arg518, also interacting with the 4-P position, is conserved in all family members except SHIP1 and SHIP2, which, as discussed above, have an insertion in this region. Together, this also suggests that the 4-P recognition is similar in most of the family members.

Membrane Interaction by Human 5-Phosphatase Catalytic Domains

Although the membrane localization of the human 5-phosphatases is often assisted by interactions through accessory domains either directly to the membrane or to other membrane localized proteins (Astle et al., 2006), the purified catalytic domains of most human 5-phosphatases are active toward liposome-containing phosphoinositide substrates. Therefore, a specific surface of the catalytic domain has evolved to mediate these interactions. The INPP5B structure reveals an extensive hydrophobic surface in the enzyme-lipophilic substrate complexes (Figure 3C). This region contains residues belonging to LC1R and LC2R motifs (Phe312, Phe313, Met374, and Met377) that interact with the aliphatic region of the diC8PtdInsP substrates, as discussed above. In the crystal lattice, the aliphatic chains of diC8PtdInsPs from three different crystallographic related molecules interact with some of these hydrophobic residues forming a highly hydrophobic cluster (Figure 5G). Several additional potential interaction points with head groups of phospholipids, or other negatively charged lipids, are lining this potential membrane interacting region (His314, Lys308, Arg376, and Arg410). Furthermore, a sulfate ion bound to Lys308 and the backbone amide of Ser307 could mark an interaction with a phospholipid head group (Figure 5A). Together, these findings suggest that this constitutes a likely membrane-interacting region. This relatively extensive interaction surface suggests that the protein will penetrate into the lipid bilayer to access the substrate. The hydrophobic patch and the sequence motif defining the binding of the aliphatic moiety of the substrates to INPP5B are also present in OCRL, supporting a similar membrane interaction for OCRL.

The putative position of the membrane upon interaction with the 5-phosphatases for INPP5B-cd, SHIP2-cd, and OCRL-cd was calculated using the positioning of protein in membrane (PPM) server. The algorithm proposes the zone of interaction between a protein and a membrane by finding the region whose transfer energy between water and a lipid layer is minimal (Lomize et al., 2006, 2012). The predictions, in all cases, agree well with our hypothesis based upon visual observations of the models (Figures 5D–5F) and define the LCRs motifs as membrane-interacting regions.

As discussed above, the high degree of conservation of residues involved in 1-P, 4-P, and 5-P interactions suggest that phosphoinositides interact in the same way in most of the 5-phosphatases. For geometric reasons, it is therefore likely that similar regions of the proteins are involved in membrane interactions, albeit detailed interactions can be made quite differently. The LC1R and LC2R regions contain hydrophobic residues in most of the family members. However, SHIP1 and SHIP2 lack the region corresponding to the LC1R-motif in INPP5B, and the structure of SHIP2 confirms that no other residues are substituting for the LC1R-motif in this region. Because our activity data indicate a very low activity of the isolated SHIP2 catalytic domain on the diC8PtdInsP substrates, it might be that its activity is more dependent on the membrane binding and interactions mediated by other domains. For instance, the N-terminal SH2 domain in SHIP2 contributes to membrane localization indirectly by binding to the adaptor proteins Shc and p130CAS or directly by binding

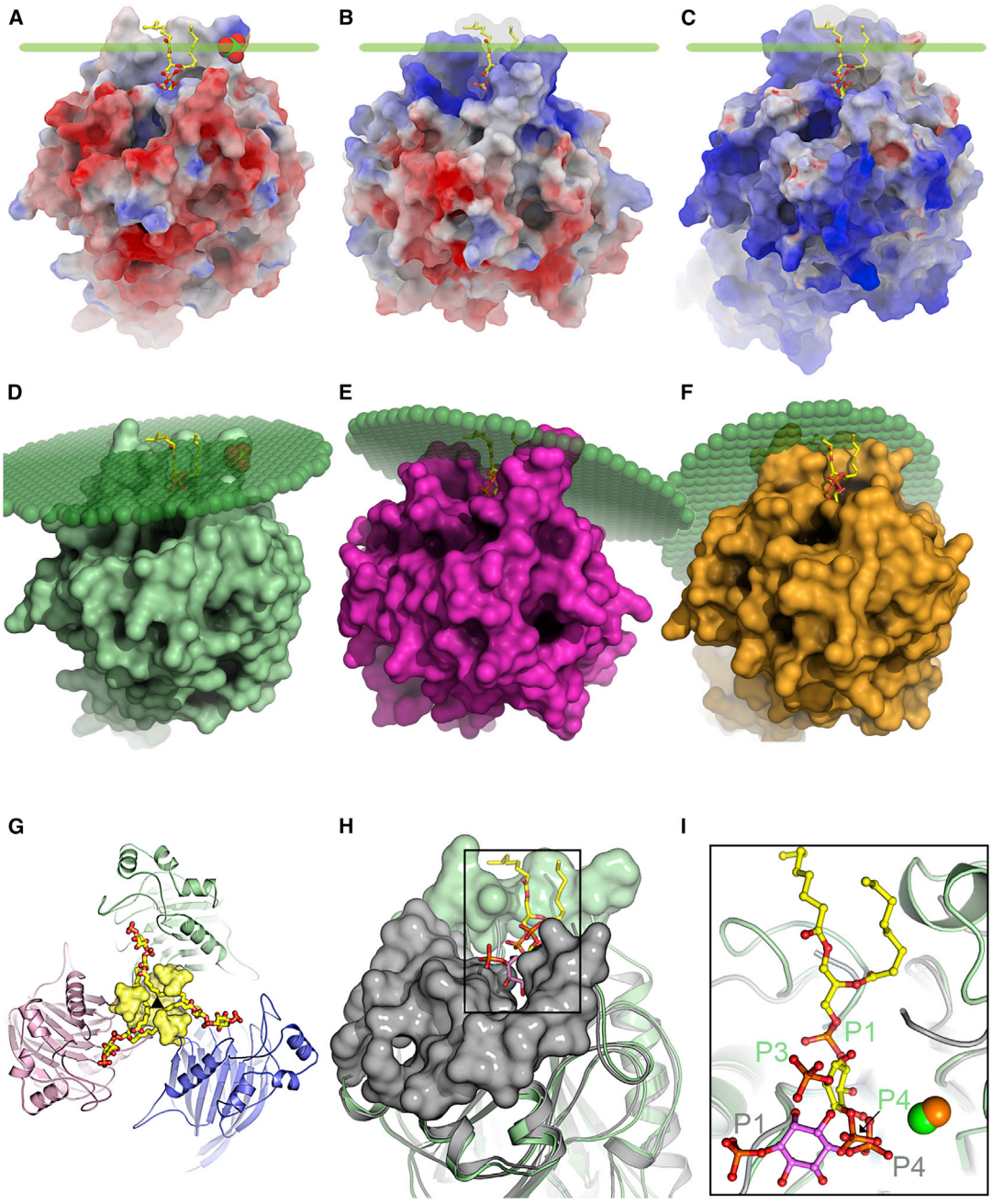

Figure 5. Structural Model of Association of 5-Phosphatases to the Membrane

(A–C) Electrostatic potential surface of INPP5B-cd bound to diC8PtdIns(3,4)P2 (A), apo-SHIP2 (B), and apo-OCRL (C). The loop encompassing residues 533–538 in SHIP2 was modeled after the corresponding loop in INPP5B-cd. Mg^{2+} ion from INPP5B-cd was also docked in the model used to compute electrostatic potentials. The molecule of diC8PtdIns(3,4)P2 is shown as a ball and sticks model, the sulfate ion as a van der Waals sphere, and the putative interaction plan with the membrane as a green line. In (B) and (C), the molecule of diC8PtdIns(3,4)P2 is issued from a superimposition between INPP5B-cd and either SHIP2-cd (B) or OCRL-cd (C).

(D–F) Location of the membrane plan determined by the PPM server for INPP5B-cd bound to diC8PtdIns(3,4)P2 (D), SHIP2-cd (E), and OCRL-cd (F). The membrane plan is represented by transparent green spheres.

(G) The 3-fold crystallographic axis constituted by the assembly of LC1R and LC2R motifs. The molecular surface of residues belonging to LC1R and LC2R motifs is yellow.

(H) Suggested membrane-interacting regions in INPP5B-cd (cyan) bound to diC8PtdIns(3,4)P2 and SPsynaptojanin-cd (gray) bound to Ins(1,4)P2. Ligands are displayed as sticks with their carbon atoms colored either yellow (diC8PtdIns(3,4)P2) or pink (Ins(1,4)P2). Residues interacting with the membrane are shown as molecular surface.

(I) Comparison between INPP5B-cd (green) and SPsynaptojanin-cd (gray) complexes with diC8PtdIns(3,4)P2 (yellow) and Ins(1,4)P2 (pink), respectively. This represents a close-up view of the boxed region on Figure 5G. Phosphate positions are labeled in green (INPP5B-cd complex) and gray (SPsynaptojanin complex). Mg^{2+} ion in INPP5B-cd is shown as an orange sphere, Ca^{2+} ion in SPsynaptojanin-cd as a green sphere.

to hepatocyte growth factor receptor c-Met (Koch et al., 2005; Prasad et al., 2001; Wisniewski et al., 1999).

DISCUSSION

Understanding the molecular details of enzymes in the PtdInsP pathways has been challenging, partly due to difficulties in structural and biochemical work on lipid- and membrane-interacting proteins. Using efficient screening techniques, we identified constructs of three human 5-phosphatases allowing high-resolution structural studies, as well as stabile complexes with lipid-like products for one of these enzymes to be generated. Conserved sequence motifs support a conserved interaction mode with the PtdInsP head group in most human 5-phosphatases, as seen in INPP5B. Consequently, similar regions of these proteins are likely to be involved in membrane interactions, and the nature of the substrate interactions in INPP5B is consistent with a model where the catalytic domain inserts slightly into the membrane to access substrates.

We note that the Ins(1,4)P2 product binding mode in the SPsynaptojanin structure is very different from that of our lipid-like PtdInsP products in INPP5B (Tsujishita et al., 2001; Figures 1C and 5I). Ins(1,4)P2 was also used as a model for interactions of SPsynaptojanin with PtdInsP, leading to the proposal of a very different membrane interacting surface to the one we observe in INPP5B (Figure 5H). The interactions of the P1 of Ins(1,4)P2 SPsynaptojanin do not involve any conserved residues and only one hydrogen bond is made, with the main chain amide of Tyr704. Because residues for PtdInsP head group interactions in INPP5B are conserved in SPsynaptojanin including P1 interactions, we feel that substrate and membrane interactions in SPsynaptojanin need to be reevaluated.

This is of a special importance to increase the chances of success of the various drug development initiatives that target the 5-phosphatase family members. For instance, small-molecule inhibitors of SHIP2 were recently shown to lower plasma glucose levels and improve glucose intolerance in diabetic mice (Annis et al., 2009; Ichihara et al., 2013; Suwa et al., 2009, 2010b). Additionally, evidence that SHIP2 and its close homolog SHIP1 act as proto-oncogenes is emerging and specific inhibitors toward this enzymes show promising effects on breast cancer and multiple myeloma models (Fuhler et al., 2012). In vitro and in vivo (on rodent models) studies have revealed the potential of AQX-1125, an activator of SHIP1, in anti-inflammatory therapy. This molecule is now in phase II clinical trials (Stenton et al., 2013a, 2013b).

In conclusion, we presented an updated model describing interactions between the 5-phosphatases and their ligands. This allowed us to identify important residues for ligand binding, catalysis, and membrane interaction. Due to the importance of the 5-phosphatases in human health, the structural and mechanistic models can support the design of specific inhibitors for a particular 5-phosphatase.

EXPERIMENTAL PROCEDURES

Protein Expression and Purification

The sequences encoding INPP5B-cd residues 262–566 (apo structure) or residues 259–563 (products complexes structures) and OCRL-cd residues 215–560 were subcloned into the vector pNIC-CH2 adding a C-terminal 6 × His-tag. The sequences encoding SYNJ1-cd residues 508–901 and SYNJ2-cd residues 506–984 were subcloned into the vector pNIC-Bsa4. The sequence encoding SHIP2-cd residues 419–832 was subcloned into the vector pNIC-MBP. In the pNIC-Bsa4 vector and pNIC-MBP vectors, an N-terminal 6 × His-tag is added to the proteins. The proteins were expressed in *Escherichia coli* and purified from the soluble fraction of the cell lysate by metal affinity chromatography followed by gel filtration. The His-tag was removed from SHIP2 by incubating with TEV protease. To remove any bound metals from the proteins, EDTA was added to the purified proteins and subsequently removed by dialysis. Detailed protocol including buffer composition is presented in the Supplemental Experimental Procedures.

Crystallization

All crystallization experiments were performed using the sitting-drop method. Protein concentrations used in the crystallization screens were 31.5, 21.7, 18, 14.7, and 17.1 mg/ml for apo-INPP5B-cd, PtdIns(4)P1-bound INPP5B-cd, PtdIns(3,4)P2-bound INPP5B-cd, SHIP2-cd, and OCRL-cd, respectively. Prior to setting up the crystallization trials, proteins were incubated on ice with either 2 mM biphenyl 2,3′,4,5′,6-pentakisphosphate (apo-INPP5B-cd), or 2 mM $MgCl_2$ and 1mM diC8PtdIns(4)P (PtdIns(4)P1-bound INPP5B-cd), or 2 mM $MgSO_4$ and diC8PtdIns(3,4)P2 (PtdIns(3,4)P2-bound INPP5B-cd), or 2 mM biphenyl 2,3′,4,5′,6-pentakisphosphate and 2 mM $MgSO_4$ (SHIP2-cd). For SHIP2-cd, the same crystal form could also be obtained without added biphenyl 2,3′,4,5′,6-pentakisphosphate. Structure determination at 3.2 Å of these crystals showed identical structure to the one with biphenyl 2,3′,4,5′,6-pentakisphosphate within experimental errors. Thus, the presence of this ligand might not have influenced the conformation of the protein especially because no residual density corresponding to it could be observed in the resulting electron density maps. Crystals were obtained by mixing 0.1 μl of precipitant with either 0.1 μl of protein solution (apo-INPP5B-cd, PtdIns(4)P1-bound INPP5B-cd and OCRL-cd) or 0.3 μl of protein solution (PtdIns(3,4)P2-bound INPP5B-cd and SHIP2-cd.) For apo-INPP5B-cd, PtdIns(4)P1- and PtdIns(3,4)P2-bound INPP5B-cd, SHIP2-cd, and OCRL-cd precipitant solutions corresponded respectively to conditions D6, G2, F10, B9, and E7 from the JCSG+ Suite (QIAGEN; detailed composition of these conditions can be found in the Supplemental Experimental Procedures section). Crystals were then transferred into a cryosolution identical to the reservoir except that both the additives used before the crystallizations experiments and 25% glycerol (ethylene-glycol for SHIP2-cd crystals) were added, and that the concentration of the precipitating agent was increased by 10%. Freezing and storage of the crystals were performed in liquid nitrogen. Experimental procedures related to X-ray data collection, processing, structure determination; and refinement are provided in the Supplemental Experimental Procedures.

Malachite Green Phosphatase Activity Assay

The enzyme activity of the metal-chelated recombinant catalytic domains of PtdIns 5-phosphatases was measured using a malachite green phosphate assay kit (BioAssay Systems). Phosphatases were incubated with 50 μM diC8PtdIns(3,4,5)P3 or diC8PtdIns(4,5)P2 at 30°C for 5 min in a buffer containing 20 mM HEPES, 300 mM NaCl, 20% glycerol, 2 mM TCEP, and 2 mM $MgCl_2$, at pH 7.5 in a volume of 25 μl. The concentration enzyme varied between different PtdIns 5-phosphatases (3–100 nM). Six microliters 10% (w/v) trichloroacetic acid was added to quench the reaction. Subsequently, 69 μl H_2O was added followed by 25 μl malachite green reagent. The mixture was allowed to develop for 30 min and the optical density at 620 nm was measured.

ACCESSION NUMBERS

The PDB accession numbers for the atomic coordinates and structure factors for INPP5B apo, INPP5B in complex with diC8PtdIns(4)P, INPP5B in complex with diC8PtdIns(3,4)P2, SHIP2, and OCRL are 3N9V, 3MTC, 4CML, 3NRS, and 4CMN, respectively.

SUPPLEMENTAL INFORMATION

Supplemental Information includes Supplemental Experimental Procedures and three figures and can be found with this article online at http://dx.doi.org/10.1016/j.str.2014.01.013.

AUTHOR CONTRIBUTIONS

C.S. and P.N. designed the experiments; L.T., C.S., S.F., M.W., T.N., S.G., and M.H. performed the experiments; L.T., C.S., and P.N. analyzed the data; and L.T., C.S., H.B., and P.N. wrote the paper.

ACKNOWLEDGMENTS

We gratefully acknowledge the staffs of the ESRF (Grenoble, France), BESSY (Berlin, Germany), DIAMOND (UK), and Max-Lab (Lund, Sweden) synchrotron facilities for assistance with X-ray data collection. We thank Aled Edwards and Marina Siponen for critically reading the manuscript. This work was supported by grants from the Swedish Research Council and the Swedish Cancer Society (to P.N.). The Structural Genomics Consortium is a registered charity (no. 1097737) that receives funds from the Canadian Institutes for Health Research, the Canadian Foundation for Innovation, Genome Canada through the Ontario Genomics Institute, GlaxoSmithKline, Karolinska Institutet, the Knut and Alice Wallenberg Foundation, the Ontario Innovation Trust, the Ontario Ministry for Research and Innovation, Merck & Co., Inc., the Novartis Research Foundation, the Swedish Agency for Innovation Systems, the Swedish Foundation for Strategic Research, and the Wellcome Trust.

Received: November 8, 2013
Revised: January 24, 2014
Accepted: January 24, 2014
Published: April 3, 2014

REFERENCES

Amoasii, L., Hnia, K., and Laporte, J. (2012). Myotubularin phosphoinositide phosphatases in human diseases. Curr. Top. Microbiol. Immunol. *362*, 209–233.

Annis, D.A., Cheng, C.C., Chuang, C.C., McCarter, J.D., Nash, H.M., Nazef, N., Rowe, T., Kurzeja, R.J., and Shipps, G.W., Jr. (2009). Inhibitors of the lipid phosphatase SHIP2 discovered by high-throughput affinity selection-mass spectrometry screening of combinatorial libraries. Comb. Chem. High Throughput Screen. *12*, 760–771.

Astle, M.V., Seaton, G., Davies, E.M., Fedele, C.G., Rahman, P., Arsala, L., and Mitchell, C.A. (2006). Regulation of phosphoinositide signaling by the inositol polyphosphate 5-phosphatases. IUBMB Life *58*, 451–456.

Astle, M.V., Horan, K.A., Ooms, L.M., and Mitchell, C.A. (2007). The inositol polyphosphate 5-phosphatases: traffic controllers, waistline watchers and tumour suppressors? Biochem. Soc. Symp. 161–181.

Attree, O., Olivos, I.M., Okabe, I., Bailey, L.C., Nelson, D.L., Lewis, R.A., McInnes, R.R., and Nussbaum, R.L. (1992). The Lowe's oculocerebrorenal syndrome gene encodes a protein highly homologous to inositol polyphosphate-5-phosphatase. Nature *358*, 239–242.

Azzedine, H., Bolino, A., Taïeb, T., Birouk, N., Di Duca, M., Bouhouche, A., Benamou, S., Mrabet, A., Hammadouche, T., Chkili, T., et al. (2003). Mutations in MTMR13, a new pseudophosphatase homologue of MTMR2 and Sbf1, in two families with an autosomal recessive demyelinating form of Charcot-Marie-Tooth disease associated with early-onset glaucoma. Am. J. Hum. Genet. *72*, 1141–1153.

Beernink, P.T., Segelke, B.W., Hadi, M.Z., Erzberger, J.P., Wilson, D.M., 3rd, and Rupp, B. (2001). Two divalent metal ions in the active site of a new crystal form of human apurinic/apyrimidinic endonuclease, Ape1: implications for the catalytic mechanism. J. Mol. Biol. *307*, 1023–1034.

Bielas, S.L., Silhavy, J.L., Brancati, F., Kisseleva, M.V., Al-Gazali, L., Sztriha, L., Bayoumi, R.A., Zaki, M.S., Abdel-Aleem, A., Rosti, R.O., et al. (2009). Mutations in INPP5E, encoding inositol polyphosphate-5-phosphatase E, link phosphatidyl inositol signaling to the ciliopathies. Nat. Genet. *41*, 1032–1036.

Blunt, M.D., and Ward, S.G. (2012). Targeting PI3K isoforms and SHIP in the immune system: new therapeutics for inflammation and leukemia. Curr. Opin. Pharmacol. *12*, 444–451.

Bolino, A., Muglia, M., Conforti, F.L., LeGuern, E., Salih, M.A., Georgiou, D.M., Christodoulou, K., Hausmanowa-Petrusewicz, I., Mandich, P., Schenone, A., et al. (2000). Charcot-Marie-Tooth type 4B is caused by mutations in the gene encoding myotubularin-related protein-2. Nat. Genet. *25*, 17–19.

Chen, V.B., Arendall, W.B., 3rd, Headd, J.J., Keedy, D.A., Immormino, R.M., Kapral, G.J., Murray, L.W., Richardson, J.S., and Richardson, D.C. (2010). MolProbity: all-atom structure validation for macromolecular crystallography. Acta Crystallogr. D Biol. Crystallogr. *66*, 12–21.

Chi, Y., Zhou, B., Wang, W.Q., Chung, S.K., Kwon, Y.U., Ahn, Y.H., Chang, Y.T., Tsujishita, Y., Hurley, J.H., and Zhang, Z.Y. (2004). Comparative mechanistic and substrate specificity study of inositol polyphosphate 5-phosphatase Schizosaccharomyces pombe Synaptojanin and SHIP2. J. Biol. Chem. *279*, 44987–44995.

Communi, D., Lecocq, R., and Erneux, C. (1996). Arginine 343 and 350 are two active residues involved in substrate binding by human Type I D-myo-inositol 1,4,5,-trisphosphate 5-phosphatase. J. Biol. Chem. *271*, 11676–11683.

Conduit, S.E., Dyson, J.M., and Mitchell, C.A. (2012). Inositol polyphosphate 5-phosphatases; new players in the regulation of cilia and ciliopathies. FEBS Lett. *586*, 2846–2857.

Di Paolo, G., and De Camilli, P. (2006). Phosphoinositides in cell regulation and membrane dynamics. Nature *443*, 651–657.

Dyson, J.M., Kong, A.M., Wiradjaja, F., Astle, M.V., Gurung, R., and Mitchell, C.A. (2005). The SH2 domain containing inositol polyphosphate 5-phosphatase-2: SHIP2. Int. J. Biochem. Cell Biol. *37*, 2260–2265.

Eberhard, D.A., Cooper, C.L., Low, M.G., and Holz, R.W. (1990). Evidence that the inositol phospholipids are necessary for exocytosis. Loss of inositol phospholipids and inhibition of secretion in permeabilized cells caused by a bacterial phospholipase C and removal of ATP. Biochem. J. *268*, 15–25.

Erdmann, K.S., Mao, Y., McCrea, H.J., Zoncu, R., Lee, S., Paradise, S., Modregger, J., Biemesderfer, D., Toomre, D., and De Camilli, P. (2007). A role of the Lowe syndrome protein OCRL in early steps of the endocytic pathway. Dev. Cell *13*, 377–390.

Fuhler, G.M., Brooks, R., Toms, B., Iyer, S., Gengo, E.A., Park, M.Y., Gumbleton, M., Viernes, D.R., Chisholm, J.D., and Kerr, W.G. (2012). Therapeutic potential of SH2 domain-containing inositol-5′-phosphatase 1 (SHIP1) and SHIP2 inhibition in cancer. Mol. Med. *18*, 65–75.

Gamper, N., and Shapiro, M.S. (2007). Regulation of ion transport proteins by membrane phosphoinositides. Nat. Rev. Neurosci. *8*, 921–934.

Gorman, M.A., Morera, S., Rothwell, D.G., de La Fortelle, E., Mol, C.D., Tainer, J.A., Hickson, I.D., and Freemont, P.S. (1997). The crystal structure of the human DNA repair endonuclease HAP1 suggests the recognition of extra-helical deoxyribose at DNA abasic sites. EMBO J. *16*, 6548–6558.

Gräslund, S., Sagemark, J., Berglund, H., Dahlgren, L.G., Flores, A., Hammarström, M., Johansson, I., Kotenyova, T., Nilsson, M., Nordlund, P., and Weigelt, J. (2008). The use of systematic N- and C-terminal deletions to promote production and structural studies of recombinant proteins. Protein Expr. Purif. *58*, 210–221.

Hakim, S., Bertucci, M.C., Conduit, S.E., Vuong, D.L., and Mitchell, C.A. (2012). Inositol polyphosphate phosphatases in human disease. Curr. Top. Microbiol. Immunol. *362*, 247–314.

Hartwig, J.H., Bokoch, G.M., Carpenter, C.L., Janmey, P.A., Taylor, L.A., Toker, A., and Stossel, T.P. (1995). Thrombin receptor ligation and activated Rac uncap actin filament barbed ends through phosphoinositide synthesis in permeabilized human platelets. Cell *82*, 643–653.

Hellsten, E., Evans, J.P., Bernard, D.J., Jänne, P.A., and Nussbaum, R.L. (2001). Disrupted sperm function and fertilin beta processing in mice deficient in the inositol polyphosphate 5-phosphatase Inpp5b. Dev. Biol. *240*, 641–653.

Hoopes, R.R., Jr., Shrimpton, A.E., Knohl, S.J., Hueber, P., Hoppe, B., Matyus, J., Simckes, A., Tasic, V., Toenshoff, B., Suchy, S.F., et al. (2005). Dent Disease with mutations in OCRL1. Am. J. Hum. Genet. *76*, 260–267.

Ichihara, Y., Fujimura, R., Tsuneki, H., Wada, T., Okamoto, K., Gouda, H., Hirono, S., Sugimoto, K., Matsuya, Y., Sasaoka, T., and Toyooka, N. (2013). Rational design and synthesis of 4-substituted 2-pyridin-2-ylamides with

inhibitory effects on SH2 domain-containing inositol 5′-phosphatase 2 (SHIP2). Eur. J. Med. Chem. *62*, 649–660.

Jänne, P.A., Suchy, S.F., Bernard, D., MacDonald, M., Crawley, J., Grinberg, A., Wynshaw-Boris, A., Westphal, H., and Nussbaum, R.L. (1998). Functional overlap between murine Inpp5b and Ocrl1 may explain why deficiency of the murine ortholog for OCRL1 does not cause Lowe syndrome in mice. J. Clin. Invest. *101*, 2042–2053.

Jefferson, A.B., and Majerus, P.W. (1996). Mutation of the conserved domains of two inositol polyphosphate 5-phosphatases. Biochemistry *35*, 7890–7894.

Koch, A., Mancini, A., El Bounkari, O., and Tamura, T. (2005). The SH2-domian-containing inositol 5-phosphatase (SHIP)-2 binds to c-Met directly via tyrosine residue 1356 and involves hepatocyte growth factor (HGF)-induced lamellipodium formation, cell scattering and cell spreading. Oncogene *24*, 3436–3447.

Laporte, J., Hu, L.J., Kretz, C., Mandel, J.L., Kioschis, P., Coy, J.F., Klauck, S.M., Poustka, A., and Dahl, N. (1996). A gene mutated in X-linked myotubular myopathy defines a new putative tyrosine phosphatase family conserved in yeast. Nat. Genet. *13*, 175–182.

Ligresti, G., Militello, L., Steelman, L.S., Cavallaro, A., Basile, F., Nicoletti, F., Stivala, F., McCubrey, J.A., and Libra, M. (2009). PIK3CA mutations in human solid tumors: role in sensitivity to various therapeutic approaches. Cell Cycle *8*, 1352–1358.

Lipton, A.S., Heck, R.W., Primak, S., McNeill, D.R., Wilson, D.M., 3rd, and Ellis, P.D. (2008). Characterization of Mg^{2+} binding to the DNA repair protein apurinic/apyrimidic endonuclease 1 via solid-state ^{25}Mg NMR spectroscopy. J. Am. Chem. Soc. *130*, 9332–9341.

Liu, P., Cheng, H., Roberts, T.M., and Zhao, J.J. (2009). Targeting the phosphoinositide 3-kinase pathway in cancer. Nat. Rev. Drug Discov. *8*, 627–644.

Lomize, A.L., Pogozheva, I.D., Lomize, M.A., and Mosberg, H.I. (2006). Positioning of proteins in membranes: a computational approach. Protein Sci. *15*, 1318–1333.

Lomize, M.A., Pogozheva, I.D., Joo, H., Mosberg, H.I., and Lomize, A.L. (2012). OPM database and PPM web server: resources for positioning of proteins in membranes. Nucleic Acids Res. *40* (Database issue), D370–D376.

Maffucci, T. (2012). An introduction to phosphoinositides. Curr. Top. Microbiol. Immunol. *362*, 1–42.

Mao, Y., Balkin, D.M., Zoncu, R., Erdmann, K.S., Tomasini, L., Hu, F., Jin, M.M., Hodsdon, M.E., and De Camilli, P. (2009). A PH domain within OCRL bridges clathrin-mediated membrane trafficking to phosphoinositide metabolism. EMBO J. *28*, 1831–1842.

Martin, T.F. (2001). PI(4,5)P(2) regulation of surface membrane traffic. Curr. Opin. Cell Biol. *13*, 493–499.

McCrea, H.J., and De Camilli, P. (2009). Mutations in phosphoinositide metabolizing enzymes and human disease. Physiology (Bethesda) *24*, 8–16.

Michell, R.H. (2008). Inositol derivatives: evolution and functions. Nat. Rev. Mol. Cell Biol. *9*, 151–161.

Mills, S.J., Persson, C., Cozier, G., Thomas, M.P., Trésaugues, L., Erneux, C., Riley, A.M., Nordlund, P., and Potter, B.V. (2012). A synthetic polyphosphoinositide headgroup surrogate in complex with SHIP2 provides a rationale for drug discovery. ACS Chem. Biol. *7*, 822–828.

Mol, C.D., Izumi, T., Mitra, S., and Tainer, J.A. (2000). DNA-bound structures and mutants reveal abasic DNA binding by APE1 and DNA repair coordination [corrected]. Nature *403*, 451–456.

Moses, S.A., Ali, M.A., Zuohe, S., Du-Cuny, L., Zhou, L.L., Lemos, R., Ihle, N., Skillman, A.G., Zhang, S., Mash, E.A., et al. (2009). In vitro and in vivo activity of novel small-molecule inhibitors targeting the pleckstrin homology domain of protein kinase B/AKT. Cancer Res. *69*, 5073–5081.

Oezguen, N., Schein, C.H., Peddi, S.R., Power, T.D., Izumi, T., and Braun, W. (2007). A "moving metal mechanism" for substrate cleavage by the DNA repair endonuclease APE-1. Proteins *68*, 313–323.

Oezguen, N., Mantha, A.K., Izumi, T., Schein, C.H., Mitra, S., and Braun, W. (2011). MD simulation and experimental evidence for Mg^{2}+ binding at the B site in human AP endonuclease 1. Bioinformation *7*, 184–198.

Ooms, L.M., Horan, K.A., Rahman, P., Seaton, G., Gurung, R., Kethesparan, D.S., and Mitchell, C.A. (2009). The role of the inositol polyphosphate 5-phosphatases in cellular function and human disease. Biochem. J. *419*, 29–49.

Pesesse, X., Moreau, C., Drayer, A.L., Woscholski, R., Parker, P., and Erneux, C. (1998). The SH2 domain containing inositol 5-phosphatase SHIP2 displays phosphatidylinositol 3,4,5-trisphosphate and inositol 1,3,4,5-tetrakisphosphate 5-phosphatase activity. FEBS Lett. *437*, 301–303.

Pirruccello, M., and De Camilli, P. (2012). Inositol 5-phosphatases: insights from the Lowe syndrome protein OCRL. Trends Biochem. Sci. *37*, 134–143.

Poccia, D., and Larijani, B. (2009). Phosphatidylinositol metabolism and membrane fusion. Biochem. J. *418*, 233–246.

Prasad, N., Topping, R.S., and Decker, S.J. (2001). SH2-containing inositol 5′-phosphatase SHIP2 associates with the p130(Cas) adapter protein and regulates cellular adhesion and spreading. Mol. Cell. Biol. *21*, 1416–1428.

Samuels, Y., Wang, Z., Bardelli, A., Silliman, N., Ptak, J., Szabo, S., Yan, H., Gazdar, A., Powell, S.M., Riggins, G.J., et al. (2004). High frequency of mutations of the PIK3CA gene in human cancers. Science *304*, 554.

Sasaoka, T., Wada, T., and Tsuneki, H. (2006). Lipid phosphatases as a possible therapeutic target in cases of type 2 diabetes and obesity. Pharmacol. Ther. *112*, 799–809.

Schmid, A.C., Wise, H.M., Mitchell, C.A., Nussbaum, R., and Woscholski, R. (2004). Type II phosphoinositide 5-phosphatases have unique sensitivities towards fatty acid composition and head group phosphorylation. FEBS Lett. *576*, 9–13.

Senderek, J., Bergmann, C., Weber, S., Ketelsen, U.P., Schorle, H., Rudnik-Schöneborn, S., Büttner, R., Buchheim, E., and Zerres, K. (2003). Mutation of the SBF2 gene, encoding a novel member of the myotubularin family, in Charcot-Marie-Tooth neuropathy type 4B2/11p15. Hum. Mol. Genet. *12*, 349–356.

Sleeman, M.W., Wortley, K.E., Lai, K.M., Gowen, L.C., Kintner, J., Kline, W.O., Garcia, K., Stitt, T.N., Yancopoulos, G.D., Wiegand, S.J., and Glass, D.J. (2005). Absence of the lipid phosphatase SHIP2 confers resistance to dietary obesity. Nat. Med. *11*, 199–205.

Stenton, G.R., Mackenzie, L.F., Tam, P., Cross, J.L., Harwig, C., Raymond, J., Toews, J., Chernoff, D., MacRury, T., and Szabo, C. (2013a). Characterization of AQX-1125, a small-molecule SHIP1 activator: Part 2. Efficacy studies in allergic and pulmonary inflammation models in vivo. Br. J. Pharmacol. *168*, 1519–1529.

Stenton, G.R., Mackenzie, L.F., Tam, P., Cross, J.L., Harwig, C., Raymond, J., Toews, J., Wu, J., Ogden, N., MacRury, T., and Szabo, C. (2013b). Characterization of AQX-1125, a small-molecule SHIP1 activator: Part 1. Effects on inflammatory cell activation and chemotaxis in vitro and pharmacokinetic characterization in vivo. Br. J. Pharmacol. *168*, 1506–1518.

Suwa, A., Yamamoto, T., Sawada, A., Minoura, K., Hosogai, N., Tahara, A., Kurama, T., Shimokawa, T., and Aramori, I. (2009). Discovery and functional characterization of a novel small molecule inhibitor of the intracellular phosphatase, SHIP2. Br. J. Pharmacol. *158*, 879–887.

Suwa, A., Kurama, T., and Shimokawa, T. (2010a). SHIP2 and its involvement in various diseases. Expert Opin. Ther. Targets *14*, 727–737.

Suwa, A., Kurama, T., Yamamoto, T., Sawada, A., Shimokawa, T., and Aramori, I. (2010b). Glucose metabolism activation by SHIP2 inhibitors via up-regulation of GLUT1 gene in L6 myotubes. Eur. J. Pharmacol. *642*, 177–182.

Tolias, K.F., Hartwig, J.H., Ishihara, H., Shibasaki, Y., Cantley, L.C., and Carpenter, C.L. (2000). Type Ialpha phosphatidylinositol-4-phosphate 5-kinase mediates Rac-dependent actin assembly. Curr. Biol. *10*, 153–156.

Tsujishita, Y., Guo, S., Stolz, L.E., York, J.D., and Hurley, J.H. (2001). Specificity determinants in phosphoinositide dephosphorylation: crystal structure of an archetypal inositol polyphosphate 5-phosphatase. Cell *105*, 379–389.

Tsutakawa, S.E., Shin, D.S., Mol, C.D., Izumi, T., Arvai, A.S., Mantha, A.K., Szczesny, B., Ivanov, I.N., Hosfield, D.J., Maiti, B., et al. (2013). Conserved structural chemistry for incision activity in structurally non-homologous

apurinic/apyrimidinic endonuclease APE1 and endonuclease IV DNA repair enzymes. J. Biol. Chem. *288*, 8445–8455.

Ungewickell, A., Ward, M.E., Ungewickell, E., and Majerus, P.W. (2004). The inositol polyphosphate 5-phosphatase Ocrl associates with endosomes that are partially coated with clathrin. Proc. Natl. Acad. Sci. USA *101*, 13501–13506.

Vanhaesebroeck, B., Leevers, S.J., Panayotou, G., and Waterfield, M.D. (1997). Phosphoinositide 3-kinases: a conserved family of signal transducers. Trends Biochem. Sci. *22*, 267–272.

Waugh, M.G. (2012). Phosphatidylinositol 4-kinases, phosphatidylinositol 4-phosphate and cancer. Cancer Lett. *325*, 125–131.

Whisstock, J.C., Romero, S., Gurung, R., Nandurkar, H., Ooms, L.M., Bottomley, S.P., and Mitchell, C.A. (2000). The inositol polyphosphate 5-phosphatases and the apurinic/apyrimidinic base excision repair endonucleases share a common mechanism for catalysis. J. Biol. Chem. *275*, 37055–37061.

Wisniewski, D., Strife, A., Swendeman, S., Erdjument-Bromage, H., Geromanos, S., Kavanaugh, W.M., Tempst, P., and Clarkson, B. (1999). A novel SH2-containing phosphatidylinositol 3,4,5-trisphosphate 5-phosphatase (SHIP2) is constitutively tyrosine phosphorylated and associated with src homologous and collagen gene (SHC) in chronic myelogenous leukemia progenitor cells. Blood *93*, 2707–2720.

Yin, Y., and Shen, W.H. (2008). PTEN: a new guardian of the genome. Oncogene *27*, 5443–5453.

Zhang, Y.Q., Wang, F., Ding, J., Yan, H., and Yang, Y.L. (2013). Novel OCRL mutations in Chinese children with Lowe syndrome. World J. Pediatr. *9*, 53–57.

